Applying the Retro-Enantio Approach to Obtain a Peptide Capable of Overcoming the Blood–Brain Barrier

Roger Prades, Benjamí Oller-Salvia, Susanne M. Schwarzmaier, Javier Selva, María Moros, Matilde Balbi, Valeria Grazú, Jesus M. de La Fuente, Gustavo Egea, Nikolaus Plesnila, Meritxell Teixidó,* and Ernest Giralt*

Abstract: The blood–brain barrier (BBB) is a formidable physical and enzymatic barrier that tightly controls the passage of molecules from the blood to the brain. In fact, less than 2% of all potential neurotherapeutics are able to cross it. Here, by applying the retro-enantio approach to a peptide that targets the transferrin receptor, a full protease-resistant peptide with the capacity to act as a BBB shuttle was obtained and thus enabled the transport of a variety of cargos into the central nervous system.

Significant advances in the field of shuttle-mediated drug delivery have been made in the last decade. However, the treatment of brain disorders continues to be a challenge because of the presence of the blood–brain barrier (BBB), a highly specialized and restrictive biological barrier that insulates the central nervous system (CNS) from the other parts of the body, thus providing an optimal environment for neuronal function. The transport of compounds from the blood to the brain are hampered by the presence of tight junctions between endothelial cells in brain capillaries, low vesicular transport, high metabolic activity, and the presence of an extensive variety of efflux pumps in the lumen of brain capillaries that prevent many xenobiotics and hydrophobic compounds from accumulating in the CNS.[1] The restrictive nature of the BBB is so strong and efficient that a number of invasive strategies have been developed to tackle the delivery of drugs to the CNS. However, these approaches are potentially harmful and in some cases inefficient. Moreover, they are not suitable for chronic treatments.[2]

Despite the presence of the BBB, the brain is not fully insulated. This organ requires essential nutrients and ions to carry out its activity and to maintain CNS homeostasis. These nutrients are supplied by a number of specialized endogenous transport mechanisms located at the BBB and are potential drug-delivery gates for therapeutic treatments of CNS disorders.[2,3] Among them, receptor-mediated transcytosis is known to be suitable for the transport of large therapeutic agents, since it is vesicular-based, in addition to providing selectivity, a key issue in drug targeting. However, this type of transport is limited by the presence of endogenous substrates, which usually saturate receptors under physiological conditions.[4] To circumvent this issue, we focused on a 12-amino-acid-long peptide sequence (H-THRPPMWSPVWP-NH_2) which targets the human transferrin receptor (TfR).[5] The main feature of this peptide, which was discovered by phage display, is that it interacts with the receptor at a different binding site to that of transferrin. Although the TfR is expressed in several cell types, the main advantage of using this receptor as a gateway to the CNS is that the highest TfR expression is found on the brain microvasculature,[6] where it mediates the delivery of iron to the brain.[7] In addition, the TfR shows a higher expression on the BBB than other receptors which are traditionally used for the delivery of therapeutics into the CNS, such as the low-density lipoprotein receptor.[8]

We recently reported the capacity of the presented peptide as a BBB shuttle to facilitate the transport of gold nanoparticles through the BBB.[9] However, as expected for a peptide composed exclusively of natural amino acids, it is rapidly metabolized by serum proteases, thereby resulting in a half-life in vitro of 30 minutes (Figure 1a), thus limiting its potential therapeutic use. This low metabolic stability is

[*] Dr. R. Prades, B. Oller-Salvia, Dr. M. Teixidó, Prof. E. Giralt
Institute for Research in Biomedicine
Baldiri Reixac 10, 08028 Barcelona (Spain)
E-mail: meritxell.teixido@irbbarcelona.org
ernest.giralt@irbbarcelona.org
Dr. S. M. Schwarzmaier, M. Balbi, Prof. N. Plesnila
Department of Neurodegeneration
Royal College of Surgeons in Ireland (RCSI) (Ireland)
and
Institute for Stroke and Dementia Research (ISD)
Ludwig Maximilians University Munich (Germany)
Dr. J. Selva, Prof. G. Egea
IDIBAPS, IN^{2}UB, University of Barcelona (Spain)
Dr. M. Moros, Dr. V. Grazú, Dr. J. M. de La Fuente
Instituto de Nanociencia de Aragon (INA) (Spain)
Prof. E. Giralt
Department of Organic Chemistry, University of Barcelona (Spain)

[**] We thank Dr. F. Hellal from the Institute for Stroke and Dementia Research (ISD), Ludwig Maximilians University and Dr. J. Colom-belli from the Institute for Research in Biomedicine (IRB Barcelona) for their contribution and critical advice regarding the microscope images. We also thank Marc Guiu from the IRB Barcelona for his assistance in the IVIS in vivo imaging experiments. We thank an anonymous reviewer for drawing our attention to Ref. [22], the electronic version of which was published during the preparation of this manuscript. This study was supported by grants from ARAID, MINECO-FEDER (BIO2013-40716, BFU-2009-0786, and BFU-2012-33932), and the Generalitat de Catalunya (XRB and 2014-SGR-521). B.O.-S. is supported by a "La Caixa"/IRB Barcelona fellowship. We thank FARA, FEDAES/GENEFA, and the BABEL FAMILY for support.

Supporting information for this article is available on the WWW under http://dx.doi.org/xx/xx

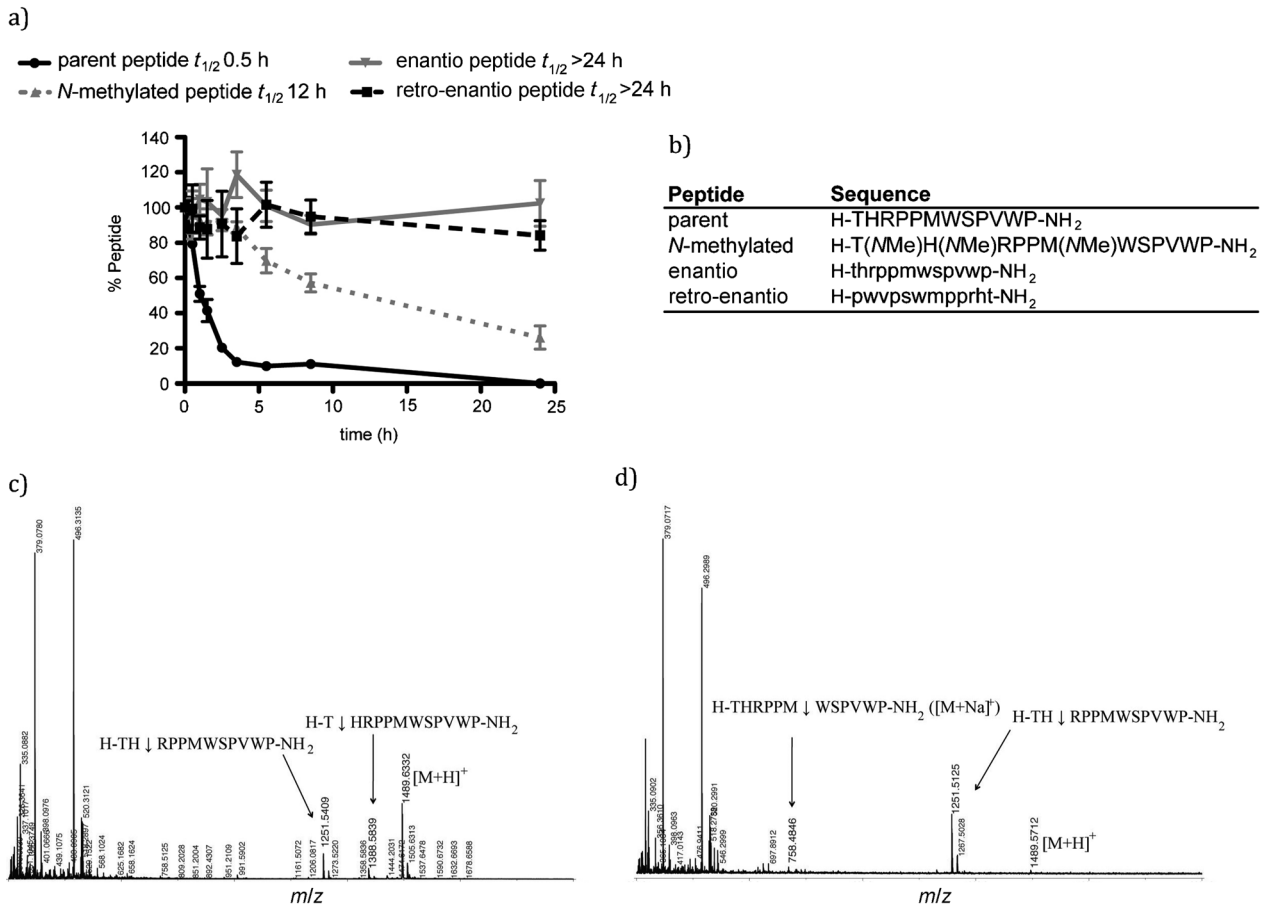

Peptide	Sequence
parent	H-THRPPMWSPVWP-NH_2
N-methylated	H-T(*N*Me)H(*N*Me)RPPM(*N*Me)WSPVWP-NH_2
enantio	H-thrppmwspvwp-NH_2
retro-enantio	H-pwvpswmpprht-NH_2

Figure 1. a) Percentage of peptide versus incubation time in human serum obtained for the parent peptide and its protease-resistant analogues: N-methylated, enantio, and retro-enantio versions. The percentage of non-metabolized peptide at each time point was determined by HPLC using a 0–50 % B gradient in 8 min (A = 0.045 % trifluoroacetic acid in water, and B = 0.036 % trifluoroacetic acid in acetonitrile). Experiments were performed in triplicate, and error bars represent the standard deviation (s.d.). b) Peptide sequences. d-Amino acids are typed in lowercase.c,d) MALDI-TOF spectra of the parent peptide after incubation with human serum for 0.5 h (c) and 1 h (d) showing the points prone to enzymatic cleavage.

a common drawback of peptides; serum proteases usually digest peptide bonds within seconds to a few minutes, thus conferring peptides with high clearance and poor pharmacokinetics. To increase the metabolic stability of the peptide under study, we *N*-methylated the positions on the peptide backbone prone to cleavage by serum proteases (Figure 1 b–d). In addition, we synthesized both the enantio and retro-enantio versions of the peptide (Figure 1 b). For these analogues, when their activity is preserved, we did not expect changes in the mechanism involved in the transcytosis of the peptides. These modifications rendered a notable increase in peptide stability (Figure 1 a). The *N*-methylated analogue showed a half-life of 12 hours in human serum, whereas the half-life of the enantio and retro-enantio versions were above 24 hours, because D-amino acids are not recognized by proteases and are therefore not processed by their machinery. With the aim to determine the impact of these modifications on the biological activity of the parent peptide, we explored the capacity of these protease-resistant analogues to interact with cells from the BBB. For this purpose, we performed cell internalization assays in brain microvascular endothelial cells and astrocytes, two basic cellular components of the BBB. A carboxyfluorescein-labeled version of the peptides was used for these experiments. After incubating the peptides for 3 hours at a concentration of 50 μM, we found that all the analogues were taken up by the selected cell lines (see Figure S4 in the Supporting Information).

After this initial checkpoint, the capacity of the synthesized protease-resistant peptides to overcome the BBB was determined in an in vitro cellular model of the BBB. This model consists of a co-culture of bovine brain endothelial cells and rat astrocytes in a porous membrane of a transwell (see Figure S5).[10] Under highly specific culture conditions, the endothelial cells of this model show tight junctions between them, become polarized, have proteolytic activity, and express efflux pumps, thus resembling the BBB. For the purposes of the experiments, the co-cultured cell barrier showed an average transendothelial electrical resistance (TEER) of $(141 \pm 6)\ \Omega\,cm^2$ before the assays, which is indicative of the tightness of the barrier. In the permeability experiments, peptides (at a concentration of 50 μM) were placed in the apical compartment of the BBB model and incubated for 2 hours. The content of the apical and basal

compartments was then analyzed by HPLC and mass spectrometry (MALDI-TOF) to determine the apparent permeability (Papp),[11] percentage of peptide transport, and peptide integrity. To assess the integrity of the cell barrier during assays, Lucifer yellow (20 μM) was co-incubated with the peptides as an internal control. According to the Lucifer yellow Papp, paracellular leakage was minimal during the experiments, thereby indicating the absence of fenestration in the cell barrier and the lack of cytotoxicity of the peptides at the concentrations tested.[12] Therefore, the transport measured during the permeability assay was attributable mainly to a transcellular mechanism.

Using this in vitro BBB model, the retro-enantio version showed almost a twofold increase in permeability (Papp of $21.4 \pm 3.8 \times 10^{-6}$ cm s^{-1}, 25.1 ± 3.0% of transport) compared with the parent peptide (Papp of $12.2 \pm 3.2 \times 10^{-6}$ cm s^{-1}, 14.9 ± 2.5% of transport). The *N*-methylated and enantio versions showed practically the same permeability as the parent peptide (Table 1). These results are consistent with the secondary structure adopted by the analogues (Figure 2). The

Table 1: Permeability of the parent peptide and its protease-resistant analogues across the cellular BBB model. N = 5. Transport was confirmed by MALDI-TOF. Data are expressed as the mean standard deviation (s.d.).

Peptide	Papp ($\times 10^{-6}$ cm s^{-1})	% Transport
parent	12.5 ± 3.4	14.9 ± 2.5
N-methylated	9.9 ± 1.6	11.7 ± 6.4
enantio	14.5 ± 2.0	17.2 ± 1.2
retro-enantio	21.4 ± 2.8	25.1 ± 3.0

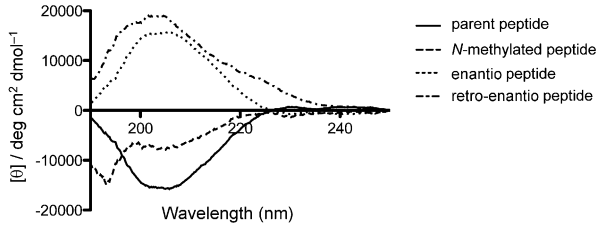

Figure 2. Circular dichroism trace of the parent peptide and its protease-resistant analogues: N-methylated, enantio, and retro-enantio versions. All the peptides were assayed at a concentration of 50 mm in 10 mm phosphate buffer (pH 7.4). Spectra were recorded at 25 8C.

parent peptide probably adopts a polyproline II conformation with a negative band at around $\lambda = 197$ nm and a positive band at $\lambda = 227$ nm.[13] This structure is preserved for the enantio version of the peptide while it is partially conserved by the retro-enantio one. The introduction of *N*-methyl groups on the peptide backbone completely disturbs the secondary structure of the latter. The enantio version is fully stable to proteases, thus influencing its bioavailability. However, as this version is the mirror image of the parent peptide, it may not be recognized properly by the TfR. Nonetheless, the balance between these two factors allows this version to cross the in vitro BBB model. The results for the *N*-methylated peptide are along the same line of reasoning. Conversely, the retro-enantio peptide has almost the same topochemical shape as the parent peptide. This feature, together with high proteolytic stability, contributes to the notable improvement in the permeability of this version across the in vitro BBB model. To confirm this hypothesis, the apical compartments were analyzed by mass spectroscopy after the 2 hour incubation. The parent peptide showed partial degradation while the protease-resistant analogues did not (see Figure S6). In addition, we calculated the mass balance by comparing the initial amount of peptide assayed to the final amount present in the apical and basal compartments. This analysis showed that more than 39 % of the parent peptide had either been degraded or trapped inside the cells after the permeability assay, thus indicating the low bioavailability of this peptide. This pronounced decrease in bioavailability was not observed for the protease-resistant analogues. On average the mass balance was 97 % for the enantio peptide, 95 % for the retro-enantio peptide, and 81 % for *N*-methylated peptide. These data indicated that the retro-enantio peptide shows an optimal balance between stability and potency, thus making it a potential BBB-shuttle candidate. Of note, Angiopep-2,[14] which displays excellent permeability across the BBB, has a lower permeability (15.8 ± 5.8% of transport) than the retro-enantio peptide in this in vitro BBB model.

These results were validated using a commercially available in vitro BBB model (Cellial Technologies) based on the monoculture of bovine brain endothelial cells with an astrocyte-conditioned medium, instead of astrocytes,[13] in a transwell system, and comparable results were obtained.

Additional permeability experiments were performed in the cellular BBB model with the aim to elucidate the mechanism involved in the passage of the retro-enantio peptide through the cellular barrier and to explore its capacity as a BBB shuttle. Regarding the crossing mechanism, we performed permeability assays at low temperature (4 °C). Under these conditions, the permeability of the peptide was negligible after 2 hours of incubation, thereby indicating that it crosses the barrier by an energy-dependent mechanism. This result was confirmed by PAMPA (parallel artificial membrane permeability assay), a technique commonly used to predict the capacity of compounds to cross the BBB by passive diffusion.[15] The permeability of the peptide was under the detection limits in this assay, thus corroborating that transport across the in vitro BBB model is not attributable to passive diffusion. In competition assays with transferrin in the cellular model, we found that the permeability of the peptide was unaltered by the presence of the protein (50 μg mL^{-1}) after a 2 hour co-incubation. In additional experiments, the peptide was co-incubated with filipin (10 μg mL^{-1}), a macrolide antibiotic which inhibits the transcytosis of transferrin.[16] Under these conditions, filipin abrogated the permeability of the peptide, since after 2 hours of incubation Papp was negligible ($< 10^{-7}$ cm s^{-1}). These observations support the notion that the retro-enantio peptide, as expected, does not compete with transferrin and that the TfR is likely to be the receptor involved in the transport of the peptide. In addition, co-localization of the peptide with transferrin was detected using fluorescence

microscopy in the internalization assays (see Figure S7). Finally, we observed that an antibody targeting the TfR competed with the retro-enantio peptide, thus attenuating the internalization of the latter in cells, an observation which supports the hypothesis that this peptide interacts with the TfR (see Figure S8). This behavior has also been observed and reported for the parent peptide.[17]

Regarding the potential of the retro-enantio peptide as a BBB shuttle, various types of cargos were attached to its *N*-terminal, and the capacity of the constructs to cross the cellular BBB model was examined. As a case of study, we selected the following: a) two small cargos, namely 5(6)-carboxyfluorescein and L-Dopa, b) a medium-sized cargo, a peptide spanning seven amino acids in length [H-a(*N*Me)f-(D)2Nal-vlkk-NH_2] with potential applications for the treatment of Alzheimer's disease[18] (it inhibits the growth of amyloid fibrils; see Figure S10 and S11), and c) two large cargos, namely iron oxide nanoparticles suitable as contrast agents for MRI[19] and quantum dots (QDs). The small and medium-sized cargos were anchored directly on the *N*-terminal of the peptide by means of solid-phase peptide synthesis (see Figures S2 and S10). For the large cargos, multiple copies of the peptide were anchored on the particles by conjugation in solution (see Figures S12–S14).

Analysis of the acceptor compartments by HPLC, MALDI-TOF, or induced-coupled plasma mass spectrometry analysis (ICP-MS) revealed that the permeability of these cargos alone was under the detection limits in this cellular model. During the assays with the retro-enantio peptide, the small and medium-sized cargos were tested at a concentration of 50 μM, whereas iron oxide nanoparticles were assayed at 5 nM (based on the total iron content of the particles) and QDs at 30 nM (based on the amount of particles). All the constructs and the corresponding controls were placed in the apical compartments of the in vitro BBB model and incubated with the cell barrier for 2 h at 37 °C. The content of the acceptor compartments was then analyzed either by HPLC and MALDI-TOF (the peptide shuttle linked to small- or medium-sized cargos) or by ICP-MS (iron oxide nanoparticles and QDs decorated with the peptide shuttle). In these experiments, the retro-enantio peptide mediated the transport of all the selected cargos (Table 2). The permeability observed for these cargo–BBB shuttle constructs was lower than that of the retro-enantio peptide (25.1 ± 3.0 % of transport) because of the presence of the cargo. Nevertheless, transport remained high for the constructs carrying small cargos. Regarding the seven-amino acid-long and nanoparticle cargos, the retro-enantio peptide also allowed their transport across the cellular BBB model. The permeability and transport values for these large cargos labeled with the retro-enantio peptide were comparable to the permeability of large molecules such as transferrin or aprotinin, which cross the BBB by receptor-mediated transcytosis and show permeability values of 9.5×10^{-7} and 2.6×10^{-6} cm s^{-1}, respectively, across a co-culture in vitro model of the BBB.[20]

As the cellular BBB model used for the permeability assays is an in vitro approximation to the true complexity of the BBB, we next explored the capacity of the retro-enantio peptide to transport a cargo into the brain in vivo. QDs (emission at $\lambda = 605$ nm) were selected as cargo for this experiment. We aimed to detect the permeability of the QD-peptide construct in living mice using intravital two-photon microscopy.[21] The experiment was performed on C57/Bl6J mice (3 animals per group). These experiments were conducted in accordance with institutional guidelines and approved by the Government of Upper Bavaria (license number and ethical approval number 06/04), and by both the Ministry for Health and Children in Dublin, Ireland (license number B100/4169), and the Research Ethics Committee of the Royal College of Surgeons (REC number 467). After drilling a hole in the skull of the mice, we placed the animals under the microscope and intravenously administered 0.1 mL of control QDs or QDs labeled with the retro-enantio peptide at a concentration of 0.8 μM (concentrations refer to QDs). The mouse brains were continuously imaged for 90 minutes. Next, the animals were injected with FITC-dextran (0.1 mL), which emits on the green wavelength and has a restricted intravascular distribution, thereby allowing identification of brain vessels. Merging the images recorded in the green and red channels revealed co-localization of the control QDs and FITC-dextran, thus indicating that the "naked" QDs remained strictly in the intravascular space of brain capillaries (Figure 3a). However, for the QDs labeled with the retro-enantio peptide, we observed red spots outside the brain

Table 2: Permeability of the retro-enantio peptide carrying various cargos across the co-culture model of the BBB, N = 5. The permeability of the peptide construct with carboxyfluorescein/L-dopa/7-mer peptide was confirmed by MALDI-TOF. Data are expressed as the mean ± s.d.

Cargo	Papp ($\times 10^{-6}$ cm s^{-1})	% Transport
carboxyfluorescein	16.2 ± 1.3	17.1 ± 2.6
L-dopa	8.5 ± 2.1	10.1 ± 1.3
H-a(*N*Me)f-(D)2Nal-vlkk-NH_2	0.14 ± 0.01	0.20 ± 0.01
iron oxide nanoparticles	0.19 ± 0.07	0.22 ± 0.05
quantum dots	0.27 ± 0.03	0.31 ± 0.02

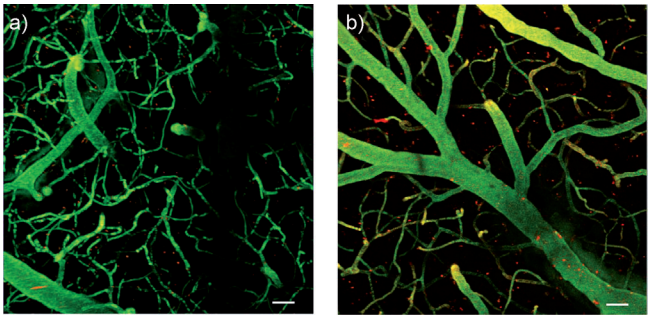

Figure 3. Intravital two-photon microscopy images of the brains of mice after injection of "naked" QDs (a) or QDs labeled with retro-enantio peptide (b). Animals were injected intravenously with the QDs and brains were imaged for 90 min. The images shown here are the compositions of merging the red channel at minute 90 after QD administration and the green channel at minute 10 after FITC-dextran administration. Images were recorded 1 mm lateral to the sagittal suture and 1 mm frontal to the coronal suture. Scale bar: 30 mm, Z-depth 200 mm.

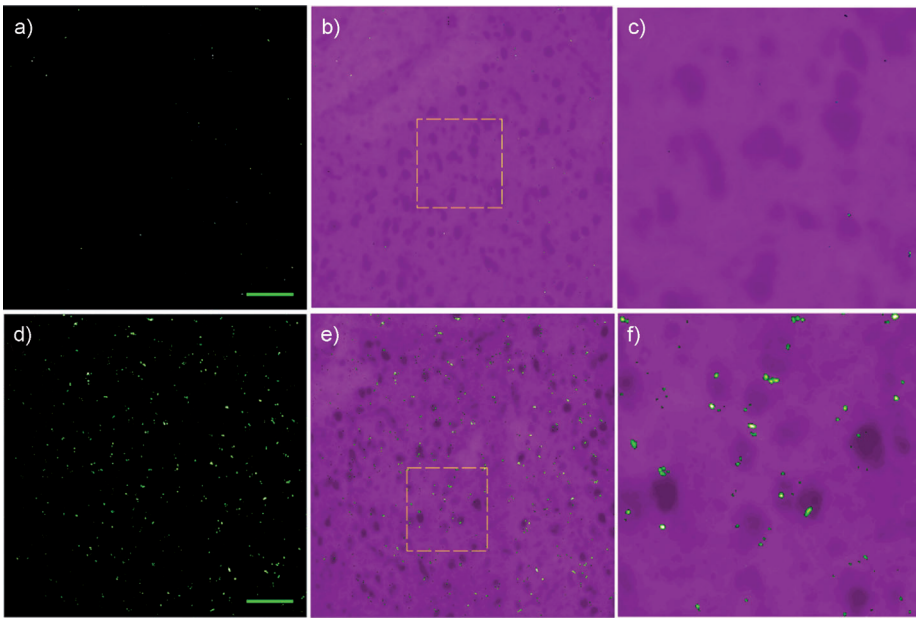

Figure 4. Ex vivo laser scanning confocal microscopy imaging of mouse brain sections (20 µm) from animals injected with "naked" QDs (a–c) or QDs labeled with retro-enantio peptide (d–f). a) Z-projection of the "naked" QD images, shown with a green-to-white look-up-table (LUT). b) Z-projection of the background fluorescence (autofluorescence, shown with a Magenta LUT) of the brain tissue, merged with image (a). The dark rounded areas are blood vessels. c) Zoomed-in image corresponding to the dashed square in B. d) Z-projection of the retro-enantio peptide labeled QD images (green-to-white LUT). e) Z-projection of the tissue (Magenta) merged with the QDs labeled with retro-enantio peptide. The dark rounded areas are blood vessels. f) Zoomed-in image corresponding to the dashed square in E. Objective 40×, scale bar: 60 µm.

vessels, thus indicating that part of the cargo–BBB shuttle system was distributed in the brain parenchyma (Figure 3b).

To confirm these results, animals were euthanized and intracardially perfused, and brain tissue was then excised. This organ was sectioned into 20 µm slices and analyzed by confocal laser scanning microscopy. The brains of animals injected with control QDs showed no isolated green spots, thus indicating that these nanoparticles did not cross the BBB (Figures 4a–c). Conversely, the brains of those injected with QDs labeled with the retro-enantio peptide showed a number of isolated green spots (Figures 4d–f), thus confirming the presence of the QDs in the brain tissue and the capacity of the retro-enantio peptide to mediate the transport of cargos across the BBB. The pattern of isolated dots observed under the microscopy is compatible with an active transport mechanism.

Finally, the efficacy of the retro-enantio peptide as a BBB shuttle was compared to that of the parent peptide, both in vitro and in vivo. For the in vitro experiments, we used the cellular BBB model and selected the following four cargos for the permeability assay: glycine, carboxyfluorescein, iron oxide nanoparticles, and QDs. These cargos were labeled either with the retro-enantio peptide or the parent peptide. After a 2 h incubation, the permeability of all the cargos was measured, and a higher permeability was observed when the cargo was linked to the protease-resistant peptide (see Figure S15 in the Supporting Information). Regarding the in vivo experiments, the parent and the retro-enantio peptides were tagged with cyanine5.5 (MW = 741.36 Da), a fluorophore suitable for in vivo imaging which was used here as a cargo for the peptides (see Figure S16). These conjugates were injected intravenously to mice (4 nmol in 150 µL, 4 animals per group). Animals were imaged in vivo at several time points using an IVIS spectrum (in vivo imaging system) instrument. Both peptides accumulated in the mouse brains in a similar amount for the first time points. However, at longer time points (4 and 8 h) the accumulation of the conjugate with the retro-enantio peptide was significantly higher than that of the parent peptide (Figure 5). We next labeled with the cyanine5.5, the construct composed by the parent or the retro-enantio peptide with the β-amyloid inhibitor peptide sequence used in the previous in vitro experiments (see Figure S17). These constructs were injected intravenously into mice (4 nmol in 150 µL, 4 animals per group) and fluorescence in the

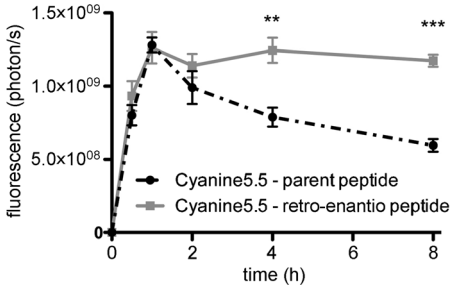

Figure 5. In vivo fluorescence quantification measured in an IVIS spectrum pre-clinical in vivo imaging system (IVIS-200) at 0.5, 1, 2, 4, and 8 h after injection. Filters were set to measure cyanine5.5 subtracting cyanine5.5 background (1 s exposure). Three groups of mice ($n = 4$) were injected with: cyanine5.5-parent peptide, cyanine5.5-retro-enantio peptide, and vehicle (sterile water). The graph plots the mean fluorescence of each group subtracting that of the vehicle at each time point. Deviation is represented as standard error mean (s.e.m.). Unpaired t student test: $^{**}P < 0.01$, $^{***}P < 0.001$.

brain was analyzed in vivo at selected time points using an IVIS spectrum. The constructs bearing the retro-enantio peptide showed a greater tendency to accumulate in the brain (see Figure S18). Taken together, these results indicate the superior performance of the retro-enantio peptide as a BBB shuttle, when compared to the parent peptide.

In conclusion, we report a protease-resistant peptide with the capacity to transport cargos of distinct sizes and types across the BBB, one of the most restrictive barriers in the

human body. In this regard, we designed this compound by applying the retro-enantio approach to a peptide that targets the TfR. This strategy has recently been successfully applied to Angiopep-2,[22] thus showing the potential of this approach. Although the terminal groups and bond direction of this peptide are reversed when compared with the parent peptide, the novel peptide showed excellent permeability, thus indicating that in this particular case these two points are minor issues. As the new peptide comprises D-amino acids, it is fully stable against proteases. In addition, it does not show toxicity and does not compete with transferrin, thus making it a suitable candidate as a BBB shuttle in clinical practice, even for chronic treatments. Moreover, because the molecule is a peptide, the risk of immunogenicity is lower than that of antibodies or proteins (also used as a BBB shuttles).[23] This potential BBB shuttle brings with it the possibility to fulfil an unmet clinical need, namely the treatment of CNS disorders.

Received:
Published online: ■■ ■■, ■■■■

Keywords: blood–brain barrier · enantioselectivity · membranes · peptides · receptors

[1] M. Demeule, A. Regina, J. Jodoin, A. Laplante, C. Dagenais, F. Berthelet, A. Moghrabi, R. Beliveau, *Vascul. Pharmacol.* **2002**, *38*, 339 – 348.
[2] M. Malakoutikhah, M. Teixido, E. Giralt, *Angew. Chem. Int. Ed.* **2011**, *50*, 7998 – 8014; *Angew. Chem.* **2011**, *123*, 8148 – 8165.
[3] R. Prades, M. Teixido, E. Giralt in *Nanostructured Biomaterials for Overcoming Biological Barriers* (Eds.: M. J. Alonso, N. S. Csaba), Royal Society of Chemistry Cambridge, **2012**, pp. 393 – 432.
[4] P. A. Seligman, *Prog. Hematol.* **1983**, *13*, 131 – 147.
[5] J. H. Lee, J. A. Engler, J. F. Collawn, B. A. Moore, *Eur. J. Biochem.* **2001**, *268*, 2004 – 2012.
[6] W. A. Jefferies, M. R. Brandon, S. V. Hunt, A. F. Williams, K. C. Gatter, D. Y. Mason, *Nature* **1984**, *312*, 162 – 163.
[7] J. R. Burdo, I. A. Simpson, S. Menzies, J. Beard, J. R. Connor, *J. Cereb. Blood Flow Metab.* **2004**, *24*, 67 – 74.
[8] Y. Uchida, S. Ohtsuki, Y. Katsukura, C. Ikeda, T. Suzuki, J. Kamiie, T. Terasaki, *J. Neurochem.* **2011**, *117*, 333 – 345; Y. Uchida, M. Tachikawa, W. Obuchi, Y. Hoshi, Y. Tomioka, S. Ohtsuki, T. Terasaki, *Fluids Barriers CNS* **2013**, *10*, 21.
[9] R. Prades, S. Guerrero, E. Araya, C. Molina, E. Salas, E. Zurita, J. Selva, G. Egea, C. Lopez-Iglesias, M. Teixido, M. J. Kogan, E. Giralt, *Biomaterials* **2012**, *33*, 7194 – 7205.
[10] P. J. Gaillard, A. G. de Boer, *Methods Mol. Biol.* **2008**, *437*, 161 – 175.
[11] P. J. Gaillard, L. H. Voorwinden, J. L. Nielsen, A. Ivanov, R. Atsumi, H. Engman, C. Ringbom, A. G. de Boer, D. D. Breimer, *Eur. J. Pharm. Sci.* **2001**, *12*, 215 – 222; V. L. Madgula, B. Avula, V. L. N. Reddy, I. A. Khan, S. I. Khan, *Planta Med.* **2007**, *73*, 330 – 335; E. S. Gil, J. Li, H. Xiao, T. L. Lowe, *Biomacromolecules* **2009**, *10*, 505 – 516.
[12] M. Culot, S. Lundquist, D. Vanuxeem, S. Nion, C. Landry, Y. Delplace, M. P. Dehouck, V. Berezowski, L. Fenart, R. Cecchelli, *Toxicol. In Vitro* **2008**, *22*, 799 – 811.
[13] I. Dalcol, M. Pons, M. D. Ludevid, E. Giralt, *J. Org. Chem.* **1996**, *61*, 6775 – 6782.
[14] M. Demeule, A. Regina, C. Che, J. Poirier, T. Nguyen, R. Gabathuler, J. P. Castaigne, R. Beliveau, *J. Pharmacol. Exp. Ther.* **2008**, *324*, 1064 – 1072.
[15] L. Di, E. H. Kerns, K. Fan, O. J. McConnell, G. T. Carter, *Eur. J. Med. Chem.* **2003**, *38*, 223 – 232.
[16] Y. Jallouli, A. Paillard, J. Chang, E. Sevin, D. Betbeder, *Int. J. Pharm.* **2007**, *344*, 103 – 109.
[17] M. Kawamoto, T. Horibe, M. Kohno, K. Kawakami, *BMC Cancer* **2011**, *11*, 359.
[18] J. Zurdo, S. Fowler, N. Carulla, E. Giralt, M. Teixido, WO/2008/050133, **2008**; D. Grillo-Bosch, N. Carulla, M. Cruz, L. Sanchez, R. Pujol-Pina, S. Madurga, F. Rabanal, E. Giralt, *ChemMedChem* **2009**, *4*, 1488 – 1494.
[19] M. Moros, B. Pelaz, P. Lopez-Larrubia, M. L. Garcia-Martin, V. Grazu, J. M. de La Fuente, *Nanoscale* **2010**, *2*, 1746 – 1755.
[20] M. P. Dehouck, P. Jolliet-Riant, F. Bree, J. C. Fruchart, R. Cecchelli, J. P. Tillement, *J. Neurochem.* **1992**, *58*, 1790 – 1797; R. Beliveau, M. Demeule, Angiochem Inc WO/2004/060403A2, **2004**; M. Demeule, J. Poirier, J. Jodoin, Y. Bertrand, R. R. Desrosiers, C. Dagenais, T. Nguyen, J. Lanthier, R. Gabathuler, M. Kennard, W. A. Jefferies, D. Karkan, S. Tsai, L. Fenart, R. Cecchelli, R. Beliveau, *J. Neurochem.* **2002**, *83*, 924 – 933.
[21] S. M. Schwarzmaier, R. Zimmermann, N. B. McGarry, R. Trabold, S. W. Kim, N. Plesnila, *J. Neuroinflammation* **2013**, *10*, 32.
[22] X. Wei, C. Zhan, X. Chen, J. Hou, C. Xie, W. Lu, *Mol. Pharm.* **2014**, *10*, 3261 – 3268.
[23] P. J. Gaillard, C. C. Visser, A. G. de Boer in *Blood – brain Barriers, Vol. 1* (Eds.: R. Dermietzel, D. Spray, M. Nedergaard), Wiley-VCH, Weinheim, **2006**, pp. 501 – 520.